Proposed Models and Methodologies for Verification Testing of AGPS-Equipped Cellular Mobile Phones in the Laboratory

Peter Boulton, Arnie Read, Spirent Communications,
Glenn MacGougan, Richard Klukas, Elizabeth Cannon, Gerard Lachapelle, University of Calgary

BIOGRAPHIES

Peter Boulton holds a Bachelors degree in Electrical and Electronic Engineering from the University of Wales at Swansea. He has been instrumental in the design, development and supply of Satellite Navigation test products for 15 years He is currently the Technical Director of the *Performance Analysis-Positioning Technology* business unit of Spirent Communications in Paignton, England, and is responsible for all product development strategy.

Arnie Read is Senior Systems Engineer at Spirent Communications with 16 years experience in satellite navigation simulation and holds a Bachelors degree in Physics from the University of London, King's College.

Glenn MacGougan is a MSc. candidate in the Department of Geomatics Engineering, University of Calgary. In 2000 he completed a BSc. in Geomatics Engineering at the same institution. He has previous experience in GPS related R&D at NovAtel Inc. and Trimble Navigation. He expects to complete his MSc in December 2002.

Dr. Richard Klukas is an Assistant Professor in the Department of Geomatics Engineering at the University of Calgary. He holds BSc and MSc degrees in Electrical Engineering and a PhD in Geomatics Engineering, all from the University of Calgary. His research interests include all aspects of wireless location.

Dr. Elizabeth Cannon is a Professor in Geomatics Engineering at the University of Calgary. She has been involved with GPS research since 1984 and has published numerous papers on static and kinematic positioning. She is a Past President of the ION.

Dr. Gerard Lachapelle holds a CRC/iCORE Chair in Wireless Location in the Department of Geomatics Engineering. He has been involved with GPS developments and applications since 1980 and has authored/co-authored numerous related publications and software. More information is available on www.geomatics.ucalgary.ca/faculty/lachap/lachap.html

ABSTRACT

This paper describes an innovative approach to the modelling of multipath impairments in a commercial laboratory test environment for mobile telephones that provide a GPS positioning capability for both emergency call location and location-based commercial services. The authors describe the background driving a need for improved laboratory representation of real-world environments that would demonstrate to regulatory authorities that extensive testing in the field is largely unnecessary, reducing vendor costs associated with qualification of multiple models of phones. Eventual standardisation of the models proposed and the test methodology would also lead to a more accurate comparison of the performance of phones from different vendors. For a field test location, results from field data are compared with those simulated for that location using the mathematical models developed.

INTRODUCTION

In the United States, the primary Location-Based Services (LBS) driver in a cellular telephone network is the E-911 mandate issued by the Federal Communications Commission (FCC), Phase II of which was due for implementation by October, 2001. This mandate requires caller location to be established in an emergency situation for 67% of mobile calls to within 50 meters and 95% of calls to within 100 meters for telephone handset-based solutions. Provision of LBS has driven the development of a number of network-based and handset-based technologies that can be used to locate the caller.

One of the handset-based technologies being adopted is Assisted-GPS (AGPS). Unlike normal GPS, the receiver does not have to extract the Ephemeris from the GPS satellite data message. This is instead provided over the phone's communication channel from a network-based resource, along with an approximate time and position. This has two major benefits. First, the phone's receiver can make a more rapid signal acquisition, as it already knows the in-view satellite candidates. Second, the receiver can make a pseudorange measurement even when the signal power is much lower than the Carrier-to-Noise ratio normally needed to read the Ephemeris data from the

navigation message without error, improving sensitivity by 25dB or more. AGPS can therefore now be used inside buildings or beneath dense foliage.

Traditionally, verification of the performance of any cellular telephone handset has relied heavily on field-testing against a reference network. While this is both costly and time consuming, the main drawback is that this can yield uncertain and variable results due to the uncontrolled nature of the test environment. Tests also cannot be repeated exactly so direct comparison is difficult. When LBS and position determination is added to the mix, the task complexity is considerably increased. The focus of the FCC is also less concerned with parametric measurement and conformance and is more about positioning performance.

The work described in this paper is a direct result of an approach to Spirent Communications by some of the leading phone vendors (Motorola, Ericsson, Nokia and Siemens). The goal was to investigate the feasibility of using sophisticated laboratory test to replace much of the need for traditional testing in the field expected by FCC 2000. These tools should provide a representative, repeatable and controlled test environment. The research and development has been conducted as a work item defined by the Location Interoperability Forum (LIF) an industry-sponsored body whose role is the establishment of various interoperability standards for mobile telephone location technologies.

RF network emulators can be used to represent both the physical communications channel and the presence, distribution and characteristics of the elements of the network that relate to the air interface such as the base stations and their associated lower level protocol stacks.

In addition, GPS simulators are fully capable of accurate replication of the signals-in-space through modelling of the satellite constellation motion and that of the handset user. In a live environment, the phone and its GPS sensor are subject to the effects of signal degradation due to path loss and, in particular, multipath. For a laboratory test to be acceptable as an alternative to live testing, the modelling of this degradation and of the location environment (urban canyon, freeway, parking garage, etc.) must be seen to be truly representative. In addition, tests must be conducted at numerous simulated locations, equivalent to 'throwing darts at a map', each of which can be essentially regarded as having a random distribution of a multipath environment.
This paper describes a test arrangement that is considered suitable for laboratory testing of the positioning capability of suitably equipped cellular telephones. The focus of the background work has been centered on the application of AGPS in a GSM or UMTS network where the position is determined within the handset, but many of the features described can also be applied to other air access technologies such as IS95 CDMA and CDMA2000.

TEST SET DESCRIPTION

The elements of the test set required for testing a GPS-enabled cell phone are shown in Figure 1. Apart from the obligatory source of GPS Signals represented by the GPS Simulator the other major item is the Air Interface Emulator (AIE). The AIE is able to emulate the mobile phone network and a base station with which the phone would communicate during a normal call. Using the communication channel, measurements made by the phone can be transferred to the test controller for analysis and test report. The same channel also supports transmission of assistance data to the cell phone. The tests system controller hosts the software components associated with control of the GPS Simulator and the AIE plus the tests scheduler and analysis tools. This is shown hosted on a single platform but could be implemented on multiple computer systems depending on the system supplier's architecture.

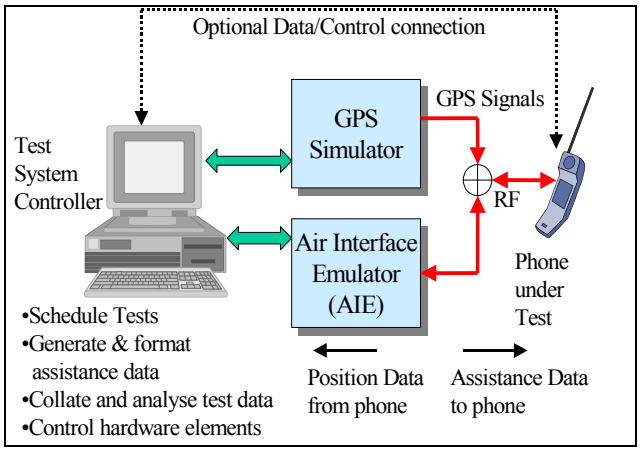

Figure 1: Cell Phone Positioning Test Set

MULTIPATH MODELLING

GPS simulators are essential test tools for all GPS-enabled user equipment as they provide a repeatable, controllable test environment and have been available for around 20 years in some form or other. Modern simulators are compact and powerful, offering a range of software features and models and the ability to generate a large number of satellite signals coherently and simultaneously. One software feature is the ability to support the generation of multipath effects. Multipath manifests itself in many ways in different applications and environments. In an airborne GPS application, for example, the multipath results from reflections from the wings or control surfaces during flight. This requires a multipath simulation model that accounts for the arrival angle of the signal at the antenna even when the aircraft is performing manoeuvres, and perhaps from ground reflections during landing. Other approaches for modelling multipath can be based on re-creating observed

and recorded variations in delay and amplitude of reflections, using polynomial data fitting. These reflected signals have required the user to manually select the satellites from the visible set that are to have a reflection associated with them according to the user's particular criterion, based on the application and the available analytical data.

These traditional analytical approaches represent a significant challenge for the user of a simulator in a land mobile application, such as a cell phone. The set of tests required to verify the positioning performance of the handset could run to many hundreds, each of which may only last for 30 seconds or so. Each would have a number of variable parameters, such as physical location and a representative environment. Here, the term 'environment' is defined to be the signal blockages due to the surrounding structures, such as trees, buildings, etc., and also localised variations relating to the conditions of use, such as a cell phone used within a car, or signal shading due to the user's head. Defining many hundreds of tests and manually selecting the satellite candidates for reflection is not really an option.

To ease the task, a new approach was devised to automatically define signal conditions by selecting from a database of pre-defined environments for each test. The analytical data relating to the delay and amplitude variation associated with the line-of-sight signals and the reflections are replaced with statistical models commonly used in laboratory testing of wireless communication equipment plus a new channel allocation algorithm.

THE NEW MODEL - FADING AND DELAY

The new multipath model assumes a GPS Simulator with between 10 and 12 channels, though 12 is considered highly desirable. Each channel can be assigned independently to represent a GPS signal with control over level, Doppler, timing and content. This includes the use of a channel to replicate a signal as an echo or reflection. The method by which channels are assigned to signals is covered after a description of the mathematics of the models applied.

The wideband Land Model Satellite (LMS) model after Jahn 2001 is generally appropriate to the GPS case. Multipath affects the timing measurement of a GPS receiver, with there being a distinct possibility of the receiver taking its pseudorange measurement against a strong, near echo instead of the line of sight (LOS) signal, which could be momentarily obscured. Advanced hardware mitigation techniques against this effect are unlikely in a cellular phone design, and so significant dilution of accuracy can be expected, especially in an urban canyon environment. The paper by Ma et al. 2001 provides real world multipath measurement data that are correlated with statistical distribution models.

Two fading models, representing amplitude noise, are employed; a Rician LOS model and a Rayleigh Echo model that in addition employs deterministic mean power reduction and deep fade models are provided for the echoes. The Rician and Rayleigh distributions with respect to mobile radio propagation are well documented and one such source is Yacoub 2000.

RICIAN LOS MODEL

The Rician model is used to describe the fading on line of sight signals. The distribution follows:

$$f_{Rician}(\nu) = 2K\nu \exp\left[-K(\nu^2+1)\right] I_0(2K\nu), v \geq 0 \quad (1)$$
$$f_{Rician}(\nu) = 0, v < 0$$

where

v	is the ratio of received voltage relative to the direct path
K	is the ratio of direct to multipath power received and is a constant, and
I_0( )	is the 0th order modified Bessel function of the first kind.

RAYLEIGH ECHO MODEL

A modified Rayleigh model is used to describe the fading on echo channels. There is a deterministic mean power function after Jahn 2001, an amplitude noise function (Rayleigh) and a delay function. The deterministic mean power reduction, in addition to Rayleigh noise, is given by:

$$P_h(\tau) = P_h(0) - d \cdot \tau \ \text{ dB} \quad (2)$$

where *Ph(0)* and *d* are provided by a look-up-table.

The amplitude noise on the echo channel, determined every user-defined iteration period, is randomly calculated to a Rayleigh distribution from Ma et al. 2001 given by:

$$f_{Rayleigh}(\nu) = 2K\nu \exp\left[-K\nu^2\right] \quad (3)$$

The user can define the iteration period (minimum 10ms with a resolution of 10ms).

The delay on the echo channel is calculated at random (from Jahn 2001) with an exponential:

$$f_{\exp}(\tau) = \frac{1}{b}\exp\left[\frac{-\tau}{b}\right] \quad (4)$$

where *b* is taken from a look-up-table. The delay is fixed for the duration of the test and the range of values generated is determined by the maximum and minimum values stored in the echo look-up table.

Deep fades occur when the summation of a set of vectors representing the reflected signals momentarily is equal in amplitude and opposite in phase to the line-of-sight signal, causing cancellation. To achieve this 'beat' effect a randomised carrier Doppler offset is applied to all echoes that have an associated line-of-sight signal. The offset is directly proportional to user speed being simulated, with a bias component to ensure that deep fades still occur even with a static user.

$$f_{coffset}(v) = B + \frac{v \cos\alpha_e}{\lambda_{L1}} \quad \text{(Hz)} \tag{5}$$

where

- λ_{L1} is the wavelength of GPS L1 frequency (m)
- **v** is the velocity being emulated, specified as part of the test definition (m/s)
- α_e is the elevation angle of the satellite, and
- **B** is the bias value for zero speed (Hz)

LOOK UP TABLES

The operation of the multipath model is controlled by the contents of a number of Look-up-Tables (LUTs), driven by satellite elevation angle and iteration rate (equivalent to simulated user speed of travel). There is a LUT for every environment type, each of which has a descriptive title; for example Urban, Suburban, Rural, Highway.

The tables can be created or edited by the user, but the default coefficients are the latest available at the time of a particular software release. As discussed in Jahn 2001, several models can be used for direct signal amplitude modulation, echo delay, echo deterministic power decay and echo amplitude modulation.

Table 1 shows an example of a Rician look-up table. Note that the categories shown are typical and additional categories are possible. The values are based on those from Ma et al. 2001.

Tables 2 and 3 show examples of Rayleigh look-up tables, with data based on Jahn 2001 and Ma et al. 2001.

Table 1 LOS Look-up table (Rician)

Type	Elevation (deg)	K
Rural	0-20	13
	20-40	35
	40-65	67
	65-90	150
Suburban	0-20	10
	20-40	20
	40-65	55
	65-90	120
Urban	0-20	5
	20-40	18
	40-65	46
	65-90	62
Highway	0-20	12
	20-40	27
	40-65	61
	65-90	135

Table 2 Maximum Delay Look-up Table for Rayleigh Model

Type	Echo Number	Delay Max (ns)
Rural	1	400
Rural	2	200
Suburban	1	400
Urban	1	600
Highway	1	600

Table 3 Echo Look-up Table (Modified Rayleigh)

Type	Elev (deg)	K Rayleigh	d Mean Loss	Ph(0) Mean Loss	b Delay
Rural	0-15	100	3	-29	0.033
	15-30	120	1	-27	0.030
	30-55	120	9.5	-25	0.027
	55-90	200	0	-100	0.010
Suburban	0-15	60	22	-22	0.037
	15-30	70	23	-23	0.039
	30-55	80	21	-25	0.030
	55-90	120	18	-24	0.033
Urban	0-15	15	11	-16	0.118
	15-30	20	25	-18	0.066
	30-55	25	7.5	-23	0.075
	55-90	50	6	-26	0.080
Highway	0-15	80	6	-27	0.072
	15-30	95	25	-26	0.084
	30-55	100	30	-27	0.067
	55-90	150	0	-80	0.010

THE NEW MODEL - SELECTING CHANNELS

The first challenge presented to the GPS simulator is the allocation of signal generator resources to the various signal requirements. GPS Simulators are equipped with a

number of physical or logical 'channels', each 'channel' representing a signal in space, either a direct line-of-sight signal from the satellite or a reflection of that signal. The number of channels available can vary from simulator to simulator, but are always finite. A typical number of channels available from a commercial simulator might be 10 or 12. However, in a real environment where multipath is present, the number of potential signals in space could be significantly larger. Therefore, any model that attempts to define the environment with finite channel resources must adopt a compromise, concentrating the resources on the properties that have the most appropriate environmental impact.

The first element of the compromise is to define four potential categories to each of the satellite signals that would be theoretically visible using a given constellation at the simulated location, assuming initially that there are no artificial blockages due to buildings, terrain etc. These categories are as follows:

Cat A. Satellites are not simulated (obscured)
Cat B. Satellites provide a direct line-of sight and are essentially not subject to obstructions or reflections (echoes)
Cat C. Satellites provide a line-of-sight but also suffer from reflections (echoes)
Cat D. Satellites only provide reflected signals (echoes)

The second stage of the compromise is to map the categories to the arrival vector of the satellite signal in terms of azimuth and elevation angle. This is achieved by defining a hemispherical category mask, centred on the simulated location and populated by the user to define the immediate environment as shown in Figure 2.

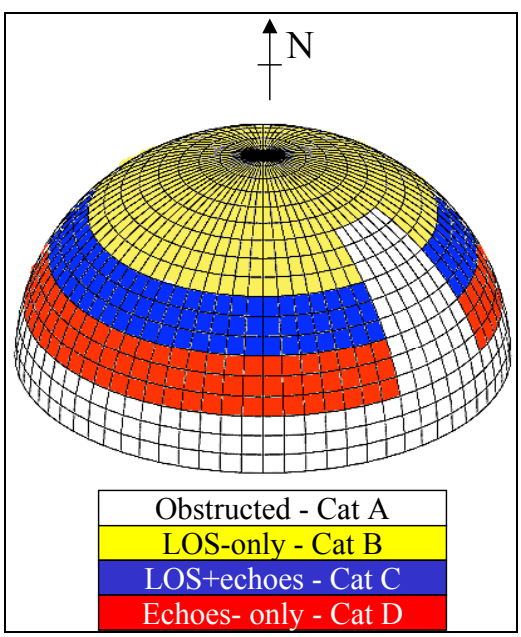

Figure 2: Category Mask

The segments of the hemispherical mask have a 5-degree resolution. Multiple masks can be defined to represent different typical environments, such as 'Urban Canyon', 'Suburban', 'Highway', etc., and these masks can be simply selected and applied as appropriate for the particular test. The simulator calculates the arrival vector of each signal and the mask acts as a look-up-table to categorise that satellite signal for the next phase of the compromise.

Once the satellite has been categorised, the final step is to map the available channel resources to the signals to be generated. There are some basic assumptions made. The first assumption is that there are more channels available than visible (unobstructed) satellites. In practice, with at least 12 channels and a typical 28-satellite GPS constellation, this is generally true, with typically 6 or 7 in view at a terrestrial location. The environment will obstruct some of these signals and they will not need to be simulated and hence will use no channel resources, leaving these available for other satellites that will generate echo signals.

The second assumption is that satellites that present a lower elevation angle are more likely to generate echoes in practice.

The channel allocation algorithm applied uses the second assumption as one of its fundamental principles.

Step 1. Any satellite vector that maps to a segment of the category mask defined as category A is excluded from selection for simulation.
Step 2. The remaining visible satellites are sorted in order of elevation.
Step 3. Starting with the lowest elevation satellite, identify its category from the mask.
Step 4. If it is category B, Line of sight (LOS) only, allocate the next available channel to this signal. Exclude this satellite from the remainder of the process since it is simulated only once (no echoes). Go back to step 3 using the next highest elevation satellite.
Step 5. If the satellite is category C (LOS plus echoes) allocate the next available channel as a LOS signal for this satellite. Keep this satellite for the rest of the process but re-categorise as category D. Go back to step 3 using the next highest elevation satellite.
Step 6. If all visible satellites have been allocated at least one channel and channels are still available, go back to Step 3 and start again with the lowest elevation satellite, allocating channels until no more are available. Note: that at this stage all satellites remaining in the process must be category D and only echo channels are allocated.

The following is a simplified worked example of the algorithm in practice. The location was arbitrarily chosen as Michigan Avenue, Chicago; N41° 52.872', W 87° 47', 100m ellipsoidal height. The time was chosen as 12 noon Thursday November 1, 2001 and the GPS constellation almanac for GPS Week 114 was downloaded in Yuma format from the US Coast Guard website. In this simple example, the Category mask angles were arbitrarily set in the following elevation bands, independent of azimuth:

0 to 25° elevation	Category A
25° to 35° elevation	Category D
35° to 70° elevation	Category C
70° to 90° elevation	Category B

Applying the mask angle criteria to the set of GPS satellites yields the fourth column in Table 4.

Table 4 Satellite Visibility (in order of elevation)

PRN	Azimuth (degrees)	Elevation (degrees)	Extent of simulation
3	-78.6	20.0	not simulated
14	-124.7	25.8	echoes only
9	105.1	46.9	LOS and echoes
17	155.0	54.9	LOS and echoes
15	-179.2	72.0	LOS only
18	18.7	73.1	LOS only

The simulator channel allocation algorithm produces the signal set shown in Table 5 for a 12-channel simulator.

Table 5 Channel Allocation

Chan	PRN	Multipath representation
1	14	Echo with modified Rayleigh fading
2	9	LOS with Rician fading
3	17	LOS with Rician fading
4	15	LOS with Rician fading
5	18	LOS with Rician fading
6	14	Second echo with modified Rayleigh fading
7	9	Echo with modified Rayleigh fading
8	17	Echo with modified Rayleigh fading
9	14	Third echo with modified Rayleigh fading
10	9	Second echo with modified Rayleigh fading
11	17	Second echo with modified Rayleigh fading
12	14	Fourth echo with modified Rayleigh fading

In this fairly harsh environment, only PRNs 15 and 18 are simulated by just one channel. All others have at least 3-channel representation while PRN14 has 4 channels.

COMBINING OTHER MODELS

GPS Simulators offer the ability to apply an attenuation mask representing the reception antenna gain pattern. This can also be employed to simulate the presence of localised environmental attenuators, where signals arriving from particular directions are subjected to an additional level of impairment. An example of this is the effect of head shading when the phone is in use. The signals passing through the user's head are subject to a loss of around 8-10dB. The antenna pattern can show a loss of this magnitude in this area. Another example could be attenuation due to trees, some forms of glass windows or the roof of a car. This is a particularly important refinement of the multipath model since the antenna gain pattern is referenced to the user's body frame, and arrival angles change as the user changes heading, for example. In contrast, the category mask is referenced to the fixed geography and is not dependent on the user's orientation.

One other refinement to the multipath model arises due to the use of antenna gain pattern modelling. The pattern attenuates all signals including echoes. If an echo were assigned the same arrival vector as the LOS signal, both would suffer the same attenuation and there would be no differential effect on the resulting signal levels. Clearly this is not what happens in practice, as some echoes are likely to have relatively high power when the LOS is partially obscured since they would arrive at the antenna from a different, unimpeded direction. To model this, the azimuth angle of all reflections is simply offset by 180 degrees, leaving the elevation angle unchanged. The echoes are now subjected to the pattern values on the opposite side of the pattern.

LAB/FIELD TEST RESULTS

Data was collected on the University of Calgary campus at a known point chosen to provide a similar signal environment as that experienced in a downtown setting. Buildings obscured the signals on the east and west sides of the location at elevation angles up to 30° and 50°, respectively. In addition, a walled walkway obscured signals arriving from the north below about 25° in elevation. The southern direction was relatively unhindered with some trees contributing to signal masking from the southwest side of the test site. Photos of the test location are shown in Figure 3 followed by an azimuth by elevation representation of the signal-masking environment determined from angular measurements from a total station. The building on the east and north side of the test site has a glass and metallic surface and is a probable source of strong specular signal reflection. The building on the west side of the site location has small windows and a rough stone textured exterior and is a probable source of diffuse signal reflection or obscuration.

Figure 3: Calgary Test Site

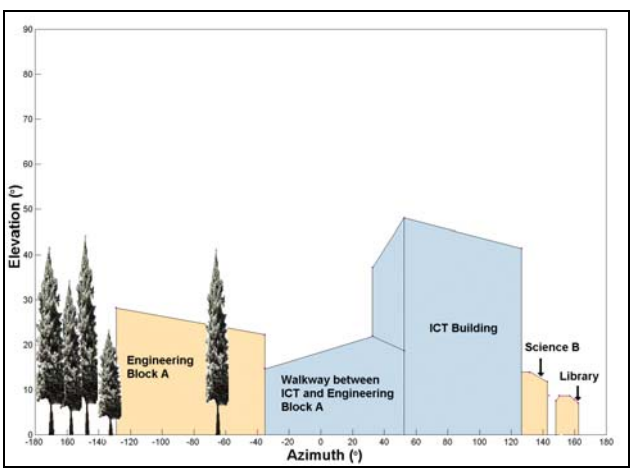

Figure 4: Representation of Calgary Test Site

Six hours of data were collected on July 04, 2002 using several GPS receivers. A low cost, high sensitivity receiver supplied by SiRF Technology (refer to MacGougan et al., 2002), typical of those to be used in cell phones, is used as the primary test receiver. In addition, receivers of the same type as the test receiver were located at a nearby reference station location with a clear view of the sky to facilitate differential measurements.

The signal attenuation at the test location was measured by differencing the test receiver carrier-to-noise density ratio data with that from the reference station receiver of similar type. This operation is shown in the following equation:

$$F = C/N_{0(reference)} - C/N_{0(rover)} \qquad \text{(dB)} \qquad (6)$$

where

F	Fading (dB)
$C/N_{0(reference)}$	Carrier to noise density ratio for the reference receiver (dB)
$C/N_{0(rover)}$	Carrier to noise density ratio for the test location receiver (dB)

This provides a good measure of the amount of signal fading at the test location. To determine the extent to which multipath and echo-only signals degrade the observations taken at the test site, the receiver's data was post-processed using parametric least squares with the position fixed to the known location. In addition, single difference corrections from the base station receiver were utilized to reduce the effect of atmospheric delays. The residuals of this solution provide a direct measure of the unmodelled effects left in the observations, namely multipath and noise. This data was binned by azimuth and elevation to provide a statistical insight into the nature of the test environment.

The mean value of the fading test measure is shown in Figure 5. The grey background lines indicate the position of the satellites as tracked by the reference station receiver. Buildings are represented by the background wire-frame. The line-of-sight signals are relatively unhindered while it is likely that strong reflections of the signals from the west were tracked and weaker reflections from the east. Intuitively, this demonstrates that the building to the east is acting as a strong specular reflector while the building to the west is acting as a weaker diffuse reflector.

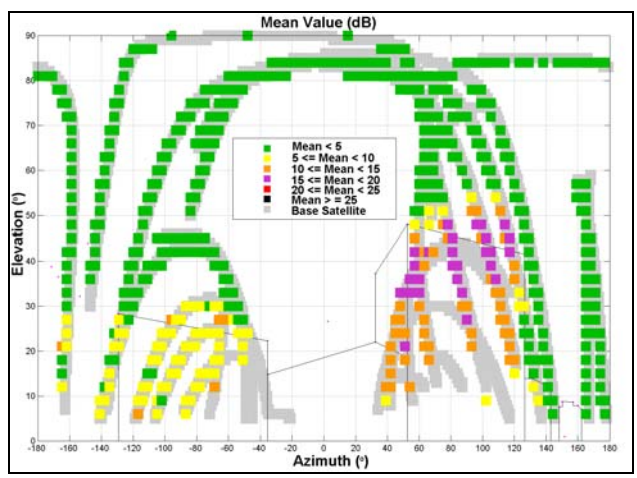

Figure 5: Signal Fading At Test Site, Fading Is Calculated As The Difference In C/N_0 Between Reference And Test Location Receivers

The root mean square (RMS) values of the position-constrained differential residuals binned by azimuth and elevation are shown in Figure 6. It should be noted that some observations were rejected from the solution and thus not included in the statistics. This was done to remove the effect of blunderous observations with residuals greater than 100m absolute. These could be due to tracking echo-only signals or possibly due to measurements of signal cross-correlation. The RMS values vary with the direction of the signal and the influence of the buildings is clear. The RMS values also decrease with increasing elevation angle.

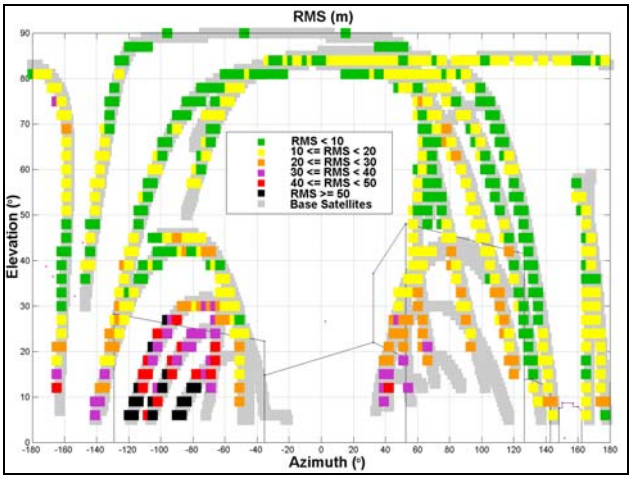

Figure 6: Residuals of Position-Constrained Differential Solution

A sample 20 minute period was chosen from the 6 hour test on July 4, 2002, for implementation and comparison with a simulation for the same location. The time series position errors for the test receiver as computed in post mission using single difference parametric least squares are shown in Figure 7. It should be noted that only the six most used satellites were used in the post-mission solution. Two other satellites provided sporadic observations. However, to simplify the ensuing simulation and ensure both the field data and simulation results refer to solutions generated using the same satellites, these two satellites were removed. Aside from a very limited fault detection method mentioned previously, no residual checking was performed for one of the post-mission solutions shown. PRN22 was identified as a problematic observation and can be removed with a simple fault detection algorithm. These results are also shown in Figure 7. The HDOP and VDOP for the post-mission solution, excluding PRN22, are shown in Figure 8. Expected error levels for simulation with and without fault detection, respectively, range from 9 meters RMS to 22-29 meters RMS horizontally and 37 meters RMS to 57-91 meters RMS vertically.

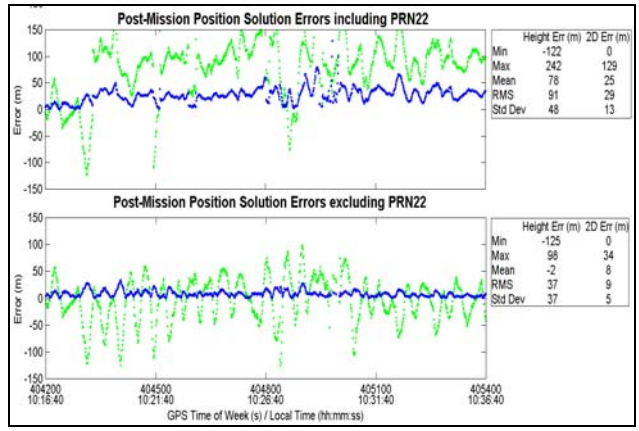

Figure 7 Position Errors With And Without PRN22 As Computed From Post-Processing Of The Test Receiver's Raw Measurements

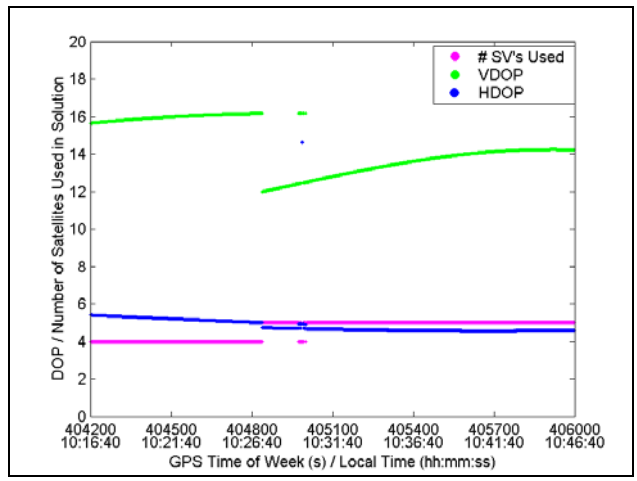

Figure 8: DOP and the Number of satellites Used in Solution, Values Calculated From the Post-Processed Solution Without PRN22

To further understand the error effects during the 20-minute test period chosen, the aforementioned constrained residual analysis was performed resulting in the values shown in Figure 9. This same data is plotted with an azimuth and elevation representation in Figure 10. Clearly the measurements of PRN22 contain very large multipath effects and/or the receiver was tracking an echo-only signal. PRN22 is located behind the building directly west of the test site and it is a fair assumption that the signal is being reflected off the highly reflective building to the east. PRN18 is located to the south of the test site where some coniferous trees are likely to mask its signal. The other satellite observations have nominal levels of error with an RMS value of approximately 8 meters.

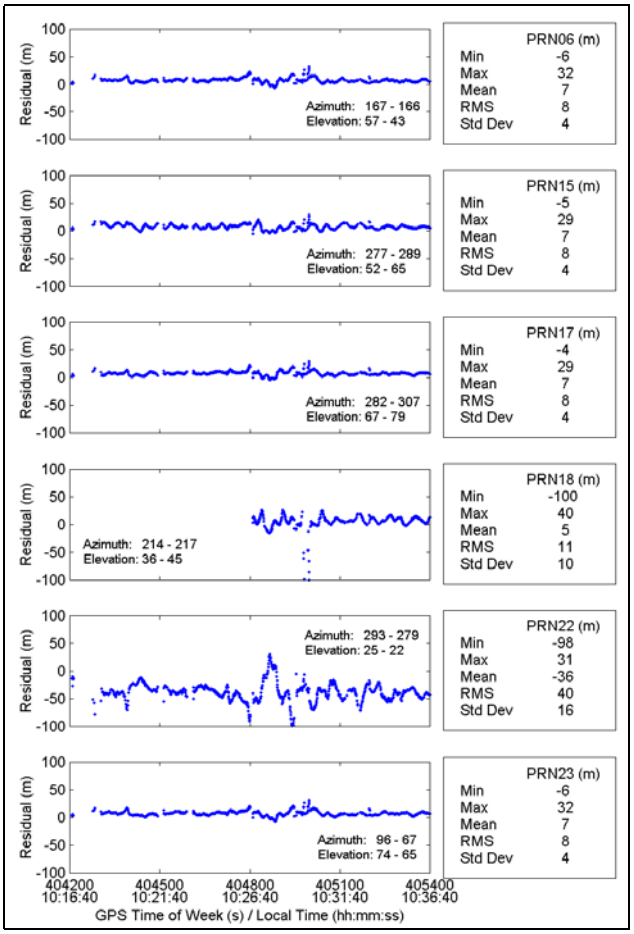

Figure 9: Time Series – Residuals Of Position-Constrained Differential Solution, Note The Large Residuals Of PRN22

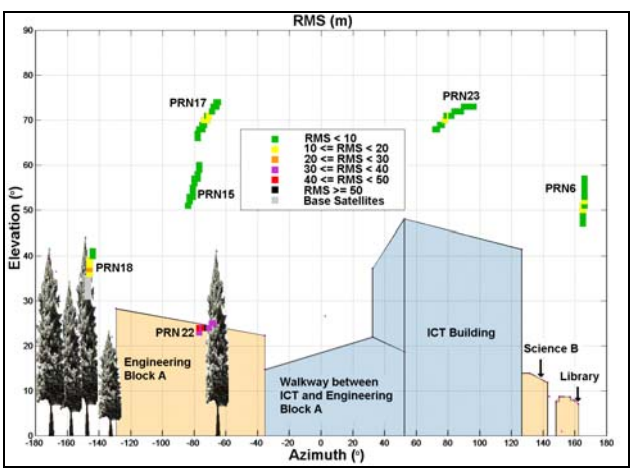

Figure 10: Residuals Of Position-Constrained Solution During Test Period, Note That Prn22 Is Behind A Building And Coniferous Trees Mask PRN18

In terms of power level degradation during the test period chosen, the time series fading data for each satellite is given in Figure 11. The expected fading levels for simulation range from 2 to 6 dB RMS for higher elevation LOS + echo signals and 8 dB RMS for low elevation LOS + echo signals and 8 dB RMS for low elevation echo-only signals. PRN22 displays some well-known interference behaviour associated with multipath and a slowly changing Doppler effect due to, in this case, satellite motion (Parsons, 1992).

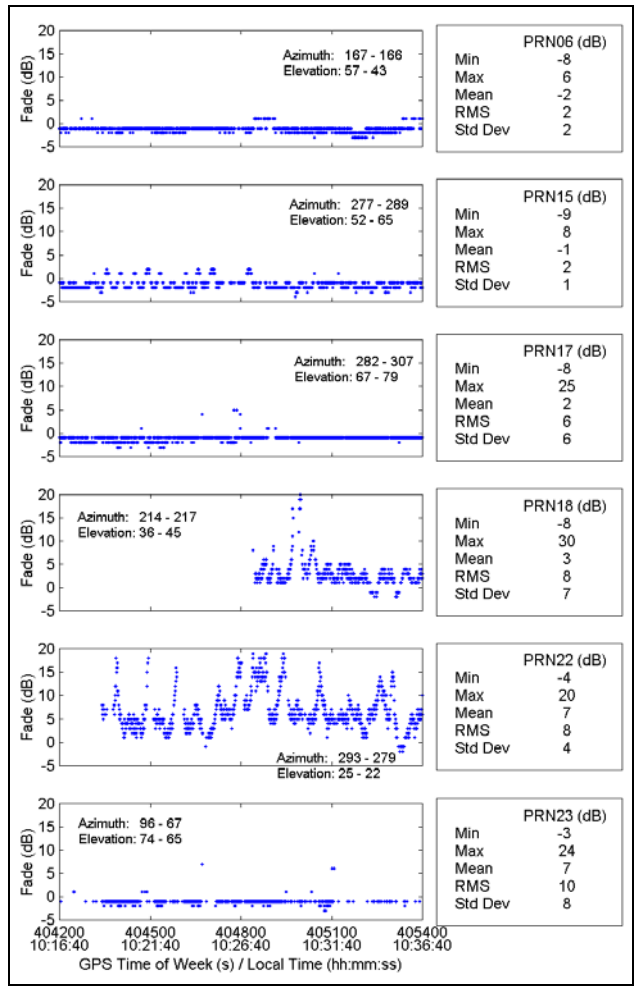

Figure 11: Signal Fading, Note The Multipath Fading Effects (Parsons, 1992) Of PRN22, Fading Is The Calculated As The Difference In C/N_0 Between Reference And Test Location Receivers

Approximate model parameters for the Rician and Rayleigh distributions, hereby referred to as the Two-State Model, were determined on a satellite-by-satellite basis using probability density data derived from the live 20-minute test data. It was found that the satellites 15, 17, 23, and 6 were distributed with almost entirely Rician distributions with high K values. Satellites 18 and 22 had distributions that followed the Rician and Rayleigh combination. The distributions for PRN 18 and PRN 22 are shown in Figures 12 and 13, respectively.

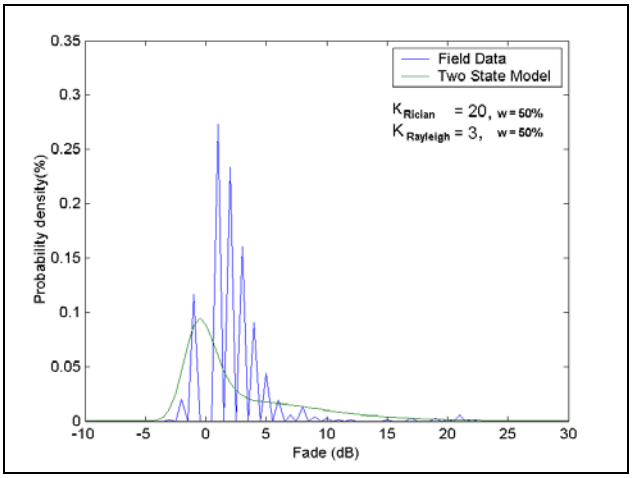

Figure 12: PRN18 – Fading Distributions For Field Data, A Two-State Model Was Fitted To The Field Data Using Empirical Methods

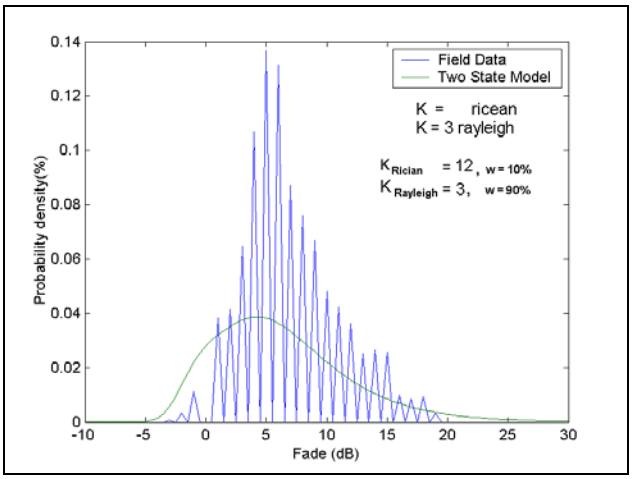

Figure 13: PRN22 – Fading Distributions for Field Data, A Two-State Model Was Fitted To The Field Data Using Empirical Methods

SIMULATION DESIGN

The real almanac for the test period, in YUMA format, was uploaded to the simulator to ensure the same constellation in both the field data and simulated data. The next task was to determine the number of satellites to simulate with the 12 available channels of the simulator. As six satellites dominated in terms of availability during the field test period, these six were chosen for simulation while all others were removed. A category mask and the aforementioned model parameters were then determined. The category mask chosen to represent the test environment is based on Figure 4 and is shown in Figure 14. The model parameters chosen were developed based on the work mentioned in Jahn 2001 and Ma et al. 2001, Figures 12 and 13, and using trial and error methods to achieve similar error and fading characteristics as discussed. The actual parameters used for the simulation discussed in this paper are shown in Figure 15.

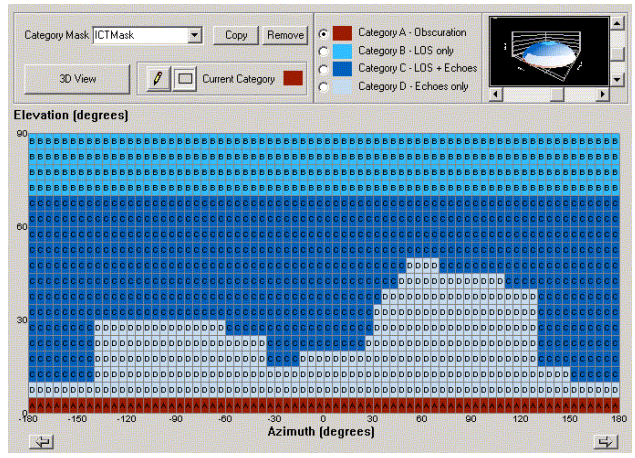

Figure 14: Simulation Category Mask

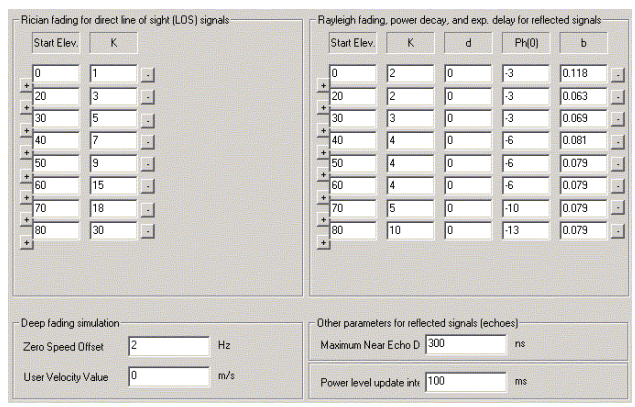

Figure 15: Simulation Model Parameters

The Rician fading parameter K was eventually chosen to be a simple linear that changes to an exponential as elevation angles increase above 50 degrees. The Rayleigh fading parameter K was chosen based on Figures 12 and 13 and using trial and error methods to achieve similar constrained residual magnitudes in comparison with the field data. These parameters are reasonable given the work presented in Ma et al. 2001 and noting that this test case is static whereas the model parameters developed in the aforementioned paper are based on kinematic data in urban environments. It is reasonable to assume that in the static case, there are lower frequency multipath effects than in the kinematic case and thus the model parameters will be different.

The model parameters chosen for the mean power reduction were simplified to the case of no additional power reduction associated with the delay value for the multipath signal, (i.e. d = 0). In addition, the values of the mean power reduction, Ph(0), were determined to provide multipath induced residuals similar to those found in the

live test. It should be noted that Ph(0) and d are much higher than the values mentioned in Jahn 2001.

The distribution parameter, b, as mentioned in one of the model equations for the distribution of the multipath delay was set at the default values. It should be mentioned that for the current simulation model, any multipath delay implemented using the Land Mobile Multipath Model is constant for the duration of the test. This is a limitation of the current model that will be discussed further when the position errors resulting from simulation are discussed.

Deep fading was arbitrarily implemented with a Zero Speed Offset of 2 Hz.

SIMULATION AND LIVE DATA COMPARISON

The simulated data collected by the test receiver was post-processed and compared to the results from the field data analysis. A comparison was made with and without fault detection and exclusion, and the time series data and statistics are presented in Figure 16. Fault detection identified PRN22 as having problematic observations and thus it was excluded from the solution. This satellite was in the echo-only category. The RMS error values for simulation and the field data are similar. However, the large amplitude sinusoidal position error behaviour of the field data could not be reproduced. This may be due to a limitation in the simulator that fixes the delay on each multipath channel for the duration of the simulation.

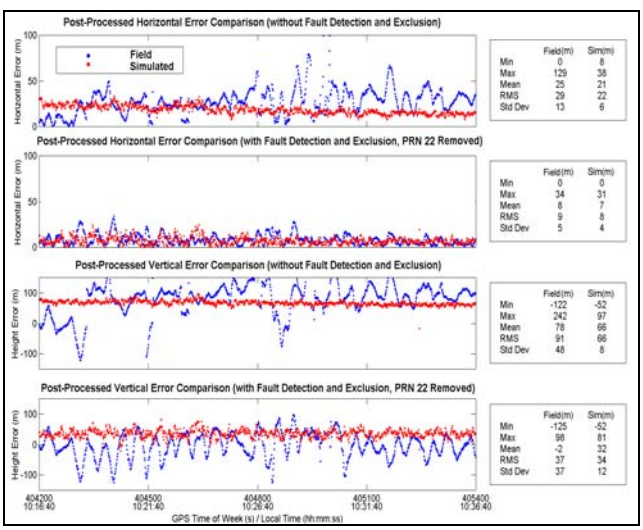

Figure 16: Position Error Comparison Between Post-Processed Receiver Measurement Data Collected In The Field And In Simulation, Results With And Without PRN22 Are Shown

The simulated data was also constrained to the true position and post-processed using parametric least squares in a manner similar to the field-data observation error analysis. The resulting residuals are compared with those from the field dataset in Figure 17. The RMS residual values are similar in magnitude but the sinusoidal behaviour of the residuals is not observed due to the fixed values of the simulated multipath delays.

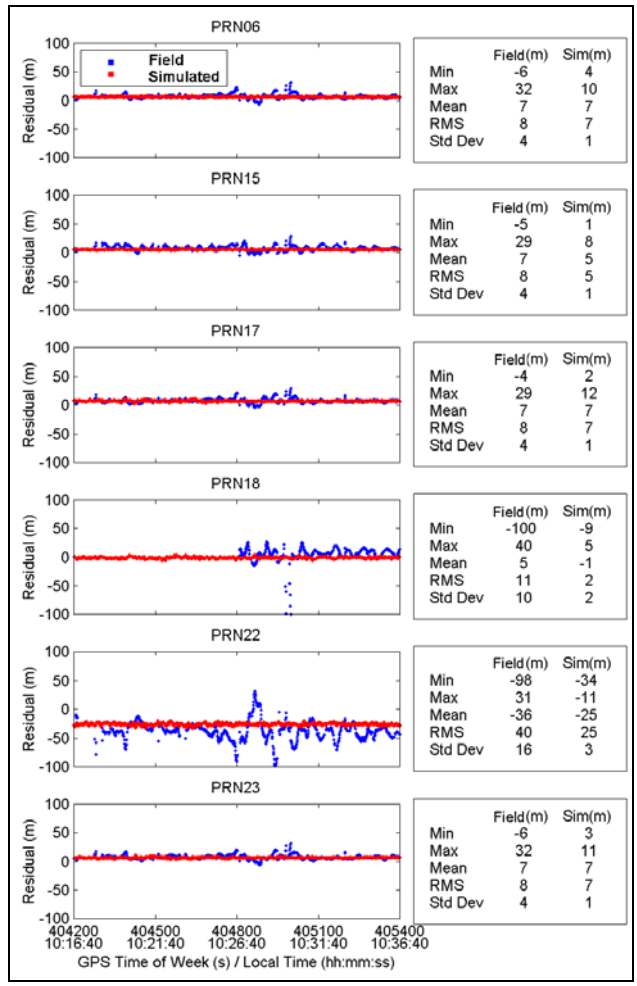

Figure 17: Comparison Of Residuals From Position Constrained Solution, As Computed From Data Collected In The Field And From Simulation

The fading values for the simulated data set were also computed. These are shown in overlay with the values from the field data in Figure 18. The statistics indicate reasonable correspondence with the field data. However, the mean fading value for PRN18 in simulation is too low and some of the deeper fades in the PRN18 and 22 field data are not observed in the simulated data.

As mentioned above, the fixed multipath delay values in the simulator may be a reason for the lack of variation in the simulated results. This is particularly true for PRN 22. During the 20 minute time period of the test data, PRN22 was dropping behind the building to the west of the test site and was simulated as Category D by the Simulation Category Mask in Figure 14. This should agree with reality in that a LOS signal from PRN22 was probably not visible at the test site. Therefore, the

discrepancy between the field and simulated results is more than likely due to the fixed delays in the simulator rather than an error in categorizing PRN22.

In the case of PRN18, however, the Simulator Category Mask used may have contributed to the discrepancy between the field and simulated results. PRN18 was rising during the 20 minutes of interest and, according to Figure 10, it was rising from behind some trees. Comparing Figure 10 to Figure 14 it is evident that the category mask did not account for these trees. It is likely that, while PRN18 was rising, reception of its LOS signal at the test site was intermittent. However, in the simulator, PRN18 was simulated as Category C – LOS and echoes – for the duration of the 20 minutes. Hence, the simulated data was, more than likely, optimistic compared to the field data.

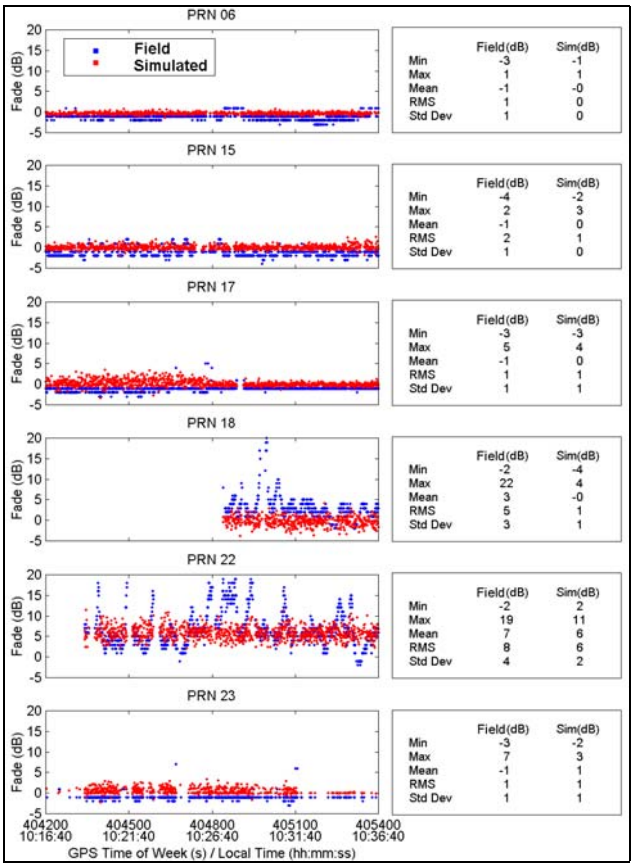

Figure 18: Fading Comparison Between Simulation Data and Field Data, Fading Is The Calculated As The Difference In C/N_0 Between Reference And Test Location Receivers

The statistical distributions of the fading values for satellites 6, 18, and 22 for the simulated data are shown in Figures 19, 19, and 20 respectively along with intuitively derived parameters for a Two State Model. Given the small sample of data, only 1200 epochs, these distributions may not have enough statistical significance to describe the distributions simulated. However, it is clear from the distribution for PRN06, which is similar to the other higher elevation LOS + echo signals simulated, that the signal received is subject to very little multipath fading. In addition, the distribution for PRN18 is curious as it provides an LOS + echo signal but has constructive interference effects that lead to higher signal powers than expected. The approximate mean fade for PRN22 is 6 dB with 2-4 dB variations.

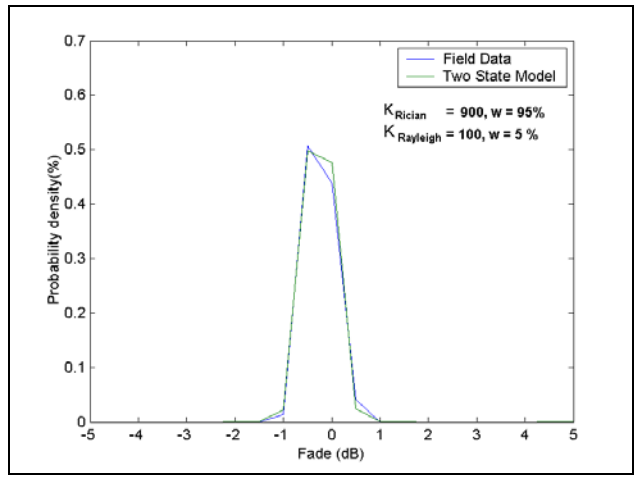

Figure 19: PRN06 – Fading Distribution for Simulated Data, A Two-State Model Was Fitted To The Field Data Using Empirical Methods

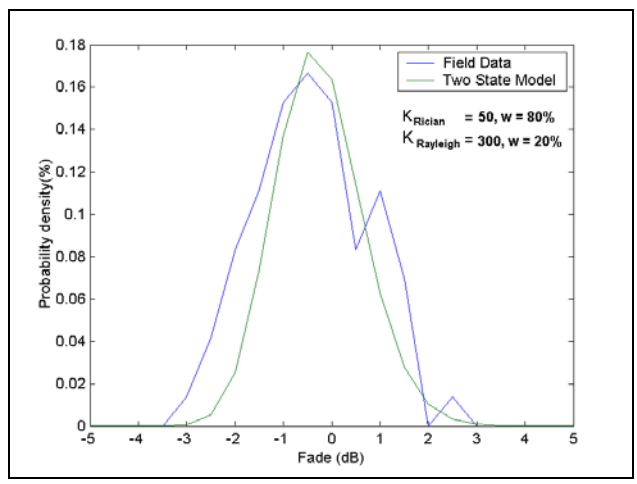

Figure 20: PRN18 – Fading Distribution for Simulated Data, A Two-State Model Was Fitted To The Field Data Using Empirical Methods

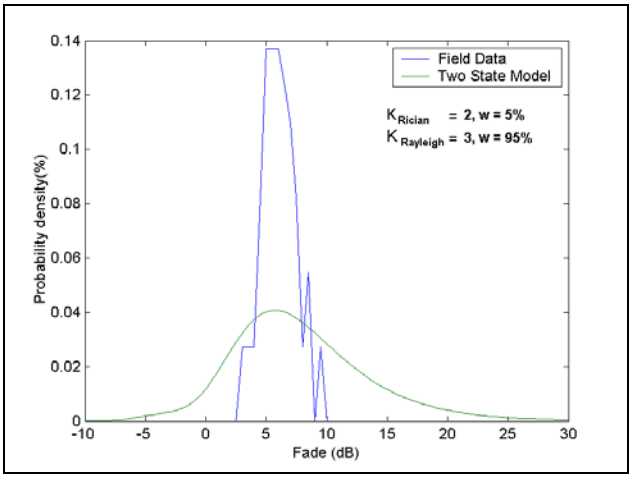

Figure 21: PRN22 – Fading Distribution for Simulated Data, A Two-State Model Was Fitted To The Field Data Using Empirical Methods

CONCLUSIONS

It was shown that the simulation model provides fading and measurement error effects, namely multipath, similar in magnitude to the field data. However, the variation of fading and multipath in terms of delay did not correspond well to the field data. Sinusoidal effects in the residuals of the position-constrained solution based on the field data were not reproduced as the delays for each multipath signal were fixed for the duration of the test. Deeper fading trends associated with PRN22 and PRN18 were also not reproduced. These variations may well be the result of signal degradation caused by the coniferous trees in the region of the signals from these PRNs. No attempt was made to adapt the category mask to the presence of these trees.

FUTURE WORK

The findings show that a variable delay function is probably required for the general use of the multipath model outside of the original E-911 requirement for many short tests. A function related to elevation angle and distance to reflector appears appropriate since lower elevation satellites will generally give the longest delays, tending to twice the distance to the reflector in the limit, and with overhead satellites provide negligible delay.

Some further investigation of the possible effects of the coniferous trees in the PRN18 and PRN22 data, combined with a variable delay model, could yield valuable insight into the modelling of these common obstructions.

This work has also not tested the validity of the use of an antenna gain pattern to modify the results in respect of effects such as head-shading of the satellite signals, in-car and in-building test cases, or the downtown urban canyon.

ACKNOWLEDGEMENTS

The efforts of Anastasia Salycheva and Eric Tong during the field and simulated data collections were instrumental in the progress of this research.

REFERENCES

Jahn, Axel (2001). Propagation Considerations and Fading Countermeasures for Mobile Multimedia Services. (May, International Journal of Satellite Communications, Vol 19, pp 223-250)

Ma, Changlin, G. Jee, G. MacGougan, G. Lachapelle, S. Bloebaum, G. Cox, L. Garin, and J. Shewfelt (2001) GPS Signal Degradation Modelling. Proceedings of the Institute of Navigation ION GPS-2001 (September 11-14, Salt Lake City, UT).

FCC (2000). Guidelines for Testing and Verifying the Accuracy of Wireless E911 Location Systems. FCC OET BULLETIN No. 71. (April 12, 2000) [http://www.fcc.gov/oet/info/documents/bulletins]

MacGougan, Glenn, G. Lachapelle, R. Klukas, K. Siu, L. Garin, J. Shewfeld, and G. Cox (2002) Degraded GPS Signal Measurements with a Stand-Alone High Sensitivity Receiver. Proceedings of National Technical Meeting, The Institute of Navigation (Jan 28-30, San Diego, CA).

Parsons, David (1992). The Mobile Radio Propagation Channel. Halsted Press, a Division of John Wiley & Sons, Inc. New York. pp. 108-130.

Yacoub, Michel Daoud (1993). Foundations of Mobile Radio Engineering. CRC Press, Inc. Boca Raton, Florida, USA. pp. 92-96.